

A RELATION BETWEEN MAGNETIC FIELD STRENGTH AND TEMPERATURE IN SUNSPOTS

GREG KOPP and DOUGLAS RABIN

National Solar Observatory, National Optical Astronomy Observatories, Tucson, AZ 85726-6732, U.S.A.*

(Received 3 January, 1992; in revised form 30 March, 1992)

Abstract. We present Stokes *I* Zeeman splitting measurements of sunspots using the highly sensitive ($g = 3$) Fe I line at $\lambda = 1.5649 \mu\text{m}$. The splittings are compared with simultaneous intensity measurements in the adjacent continuum. The relation between magnetic field strength and temperature has a characteristic, nonlinear shape in all the spots studied. In the umbra, there is an approximately linear relation between B^2 and T_b , consistent with magnetohydrostatic equilibrium in a nearly vertical field. A distinct flattening of the B^2 vs T_b relationship in the inner penumbra may be due to changes in the lateral pressure balance as the magnetic field becomes more horizontal; spatially unresolved intensity inhomogeneities may also influence the observed relation.

1. Introduction

Studies of the relationships between physical variables within sunspots have been hindered by three primary problems. First, not only do different sunspots vary widely in size and shape, there is also fine-scale spatial structure within all parts of a single spot (e.g., Livingston, 1991; Moore and Rabin, 1985). Second, because of the pervasive effect of stray light on sunspot measurements (Zwaan, 1965), many early studies are of limited value. Third, the magnetic field is not always strong enough, particularly in the penumbra, to cause complete Zeeman splitting.

Observing in the infrared alleviates the last two difficulties. Zeeman splitting as a fraction of line width increases directly with wavelength, providing three times the sensitivity at $1.56 \mu\text{m}$ as at $0.5 \mu\text{m}$. Stray light is less of a problem in the infrared than the visible for two reasons: telescope and instrument scattering is usually lower; and the effects of stray light within sunspots are small because the intrinsic intensity contrast is lower. An additional advantage of infrared observing is that it is often possible to measure a nearly true continuum intensity between spectral lines and make a straightforward estimate of temperature, while in the visible, good temperature estimation requires spectrum synthesis to account for the dense haze of umbral lines (Maltby *et al.*, 1986).

The $\lambda = 1.5649 \mu\text{m}$ (6388.6 cm^{-1}) Landé $g = 3$ Fe I triplet is formed about 110 km above the base of the quiet photosphere (Bruls, Lites, and Murphy, 1991). This line has been exploited for magnetic observations of flux tubes (Harvey and Hall, 1975; Stenflo, Solanki, and Harvey, 1987) and has been used in conjunction with infrared arrays to obtain maps of both plages (Rabin, 1992) and sunspots (McPherson, Lin, and Kuhn,

* Operated by the Association of Universities for Research in Astronomy, Inc. (AURA) under cooperative agreement with the National Science Foundation.

1992). The adjacent continuum, near the opacity minimum of the atmosphere, is formed at -30 km (Vernazza, Avrett, and Loeser, 1981). The continuum brightness temperature at $1.56 \mu\text{m}$ closely matches the kinetic temperature at the height of formation (Vernazza, Avrett, and Loeser, 1976), allowing a simple Planck-function conversion from intensity to temperature.

We report initial results from a program to map the magnetic field strength and continuum intensity of sunspots. We find a characteristic, nonlinear relation between field strength and continuum intensity.

2. Observations

2.1. INFRARED MEASUREMENTS

We obtained Stokes I profiles of six sunspots using the 81 cm east auxiliary telescope and the vertical spectrograph of the NSO McMath Telescope Facility on 13 May, 1991. The spots varied in area from 5.5 to 175 millionths of a hemisphere, and were not chosen for shape or other characteristic, except that they not be too near the limb ($\mu \geq 0.75$) (see Table I). Each spot was scanned across the slit using a precise translation stage;

TABLE I
Sunspot parameters

Region (NOAA)	Position ^a	$\mu = \cos \theta$	Area ^b	r_u^c (")	r_{pen}^c (")	$I_{u, \text{min}}/I_{ph}^d$	$I_{u, \text{ave}}/I_{\text{pen}}^d$	B_{max} (G)
6619	N29 W27	0.75	175	16.9	44.3	0.46	0.65	3510
6621	N08 W22	0.92	53	9.2	22.8	0.56	0.74	2960
6622	S27 W17	0.84	11	4.2	12.4	0.65	0.77	2630
6623	N03 W13	0.97	5.5	3.0	6.0	0.78	0.89	2270
6624	S16 E07	0.95	23	6.1	20.9	0.66	0.78	2560
6625	N10 E05	0.98	52	9.2	21.8	0.54	0.73	3090

^a Interpolated to time of observation.

^b Umbral area in millionths of a hemisphere measured from our data and corrected for foreshortening.

^c Average radius, corrected for foreshortening.

^d $I_{u, \text{min}}$ is the minimum umbral intensity; $I_{u, \text{ave}}$ the average umbral intensity; I_{ph} and I_{pen} are the mean quiet Sun (photospheric) and penumbral intensities.

overlapping spatial swaths ensured complete coverage of the penumbra and its surroundings on the larger sunspots. The 58×62 InSb infrared camera (Fowler *et al.*, 1987) co-added 20 spatial-spectral images at each slit setting. Since the grating was used in first order (incidence angle 29°), distortion of the Stokes I profile by instrumental polarization was much less than in the case of echelle-grating measurements such as those analyzed by Martínez Pillet and Sánchez Almeida (1991). The data are seeing-limited to about $2''$.

Line profiles from umbrae and penumbrae show completely split π - and σ -components of the $\lambda = 1.5649 \mu\text{m}$ Fe I line at fields stronger than 1400 G (Figure 1). The total field strength B is determined in the completely split regime from the separation of the σ -components, irrespective of field orientation. Continuum intensity I_c is measured from a quiet region of the spectrum immediately redward of the line.

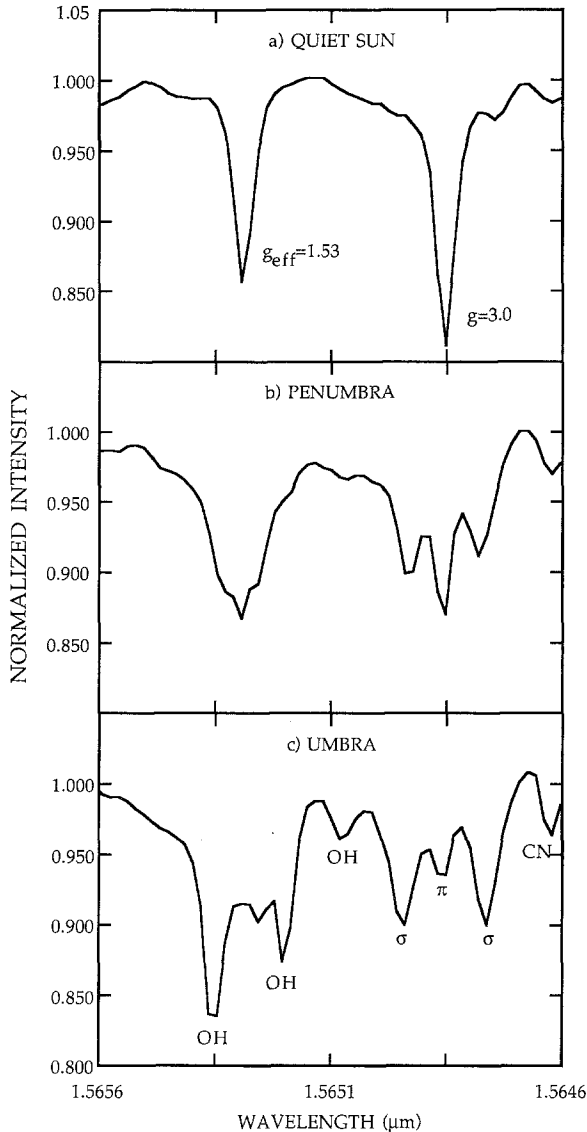


Fig. 1. Stokes I spectra of the Fe I lines at $1.5649 \mu\text{m}$ ($g = 3$) and at $1.5653 \mu\text{m}$ ($g_{\text{eff}} = 1.53$) in (a) the quiet Sun, (b) a penumbra, and (c) an umbra. The $g = 3$ line is completely split for $B \gtrsim 1400$ G. In (b), $B \approx 2150$ G; in (c) $B \approx 2600$ G. The obscuring OH lines near the $g_{\text{eff}} = 1.53$ line make it unsuitable for measuring field strengths.

At the spectral resolving power of the present observations ($\sim 4 \times 10^4$), the line profiles are adequately described by gaussians. The π - and σ -components, as well as contaminating umbral and photospheric lines, were simultaneously fitted and deblended using a nonlinear least-squares fitter. The Zeeman splitting was taken to be half the separation of the σ -components. The positions of the components could be determined to within ± 20 G in field strength units. Some spots had asymmetries between the π - and the two σ -components of up to ± 100 G; these were possibly due to a displacement of the π -component caused by an umbral blend (Solanki, 1991) and should not affect the determination of field strength from the separation of the σ -components. The uncertainty in measured continuum intensity (without stray light adjustments) is about ± 0.01 at all intensities.

Splittings in the Landé $g_{\text{eff}} = 1.53$ Fe triplet at $\lambda = 1.5653 \mu\text{m}$ (6386.9 cm^{-1}) (Solanki, Biémont, and Mürset, 1990) are not measurable because of obscuring umbral OH lines, identified by Wallace and Livingston (1992) (Figure 1(c)). We use this line for wavelength calibration only.

2.2. STRAY LIGHT

Gurman and House (1981) reported that the effect of stray light on the determination of field strength was negligible. We find the same result for the present data and have applied no corrections to the measured field strengths. We estimate the effect of stray light on the central intensities of the umbrae but make no corrections to the B vs I_c profiles presented below.

Stray light measurements were not taken at the time of observation; we therefore estimate stray light parameters from measurements taken with the McMath telescope at other times. Fortunately stray light is a less delicate problem in the infrared than in the visible, and our main results do not depend on the details of the correction.

Following the method and notation of Zwaan (1965), we model the point spread function by a Lorentzian scattering function

$$\psi_s(r) = A/(C^2 + r^2) \quad (1)$$

and a two-component blurring function

$$\psi_b(r) = (f_1/\pi b_1^2) \exp[-(r/b_1)^2] + (f_2/\pi b_2^2) \exp[-(r/b_2)^2]. \quad (2)$$

The scale length C in Equation (1) is inferred from the results of Pierce (1991), who measured the scattered light of the McMath main telescope between 1.006 and 2.0 solar radii at wavelengths out to $1.1 \mu\text{m}$. Since the scattered light decreases with wavelength, it will be conservative to apply the results at $1.1 \mu\text{m}$ to our observations at $1.56 \mu\text{m}$; this gives $C = 3.1'$. The east auxiliary telescope has the same unobstructed, all-reflecting design as the main telescope and shares its low scattered-light properties. Applying an arbitrary safety factor of five, we estimate that scattered light affected the observed umbral contrasts by at most 0.02.

Adopting a limb-darkening function given by Staveland (1972), with results interpolated for $1.565 \mu\text{m}$, we find the best fit to a limb profile obtained with the same

instrumental setup as was used for the sunspot observations to give the parameters

$$b_1 = 2.25'' , \quad b_2 = 8.5'' , \quad f_1 = 0.85 , \quad f_2 = 0.15$$

in Equation (2). We constructed a worst case by increasing the contribution of the extended gaussian as much as possible while retaining marginal agreement with the observed profile. These parameters are

$$\tilde{b}_1 = 2.0'' , \quad \tilde{b}_2 = 6.0'' , \quad \tilde{f}_1 = 0.6 , \quad \tilde{f}_2 = 0.4 .$$

Results

Figure 2 illustrates our main result: a nonlinear relation between magnetic field strength and continuum intensity within a large sunspot. The plot may be divided into three roughly linear segments: a strong variation of field with intensity above about 2500 G; a gradual change in field with a large variation in intensity from 2000–2500 G (the umbra-penumbra transition); and increased scatter and a strong change in field with intensity below 2000 G. Notice that points on opposite sides of spot center (identified by different plot symbols) define B vs I_c curves that are systematically different, particu-

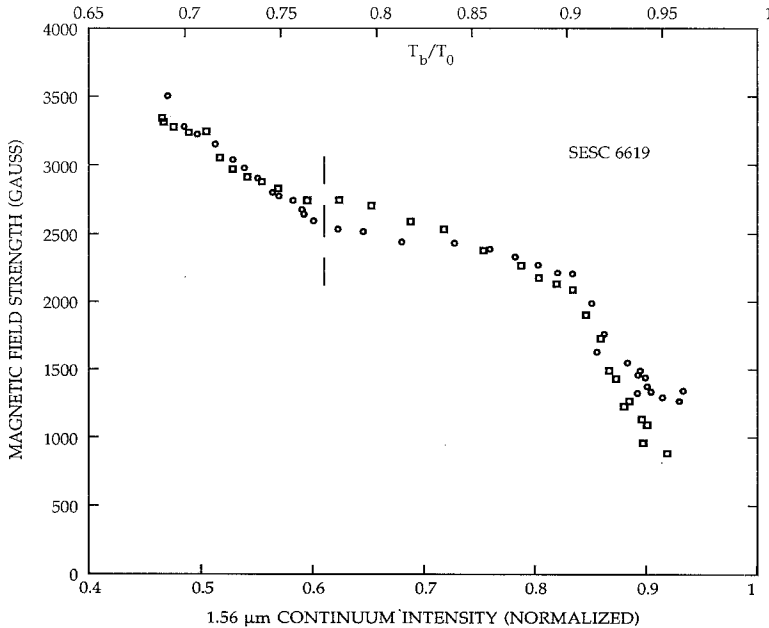


Fig. 2. Magnetic field strength vs continuum intensity across diameter of SESC 6619, 13 May, 1991. Points on opposite sides of spot center are identified by different symbols. Two distinct curves are evident, particularly near 2500 G. While the scatter in each curve is small, note the difference in field strength at a given intensity between the two. The dashed line delineates the umbral region left of which the data are nearly linear.

larly in the umbra/penumbra transition; the smoothness and consistent separation of the two curves is an external check on the uncertainties in B and I_c .

This nonlinear shape, again with intrinsic scatter, is also evident in the other spots in our sample (Figure 3). Table I presents some parameters of each observed sunspot. Although smeared somewhat by the smaller spots (which are most affected by stray light), a superposition of data from all six observed sunspots shows the consistency of this relation from spot to spot (Figure 4). Stray light corrections would decrease the

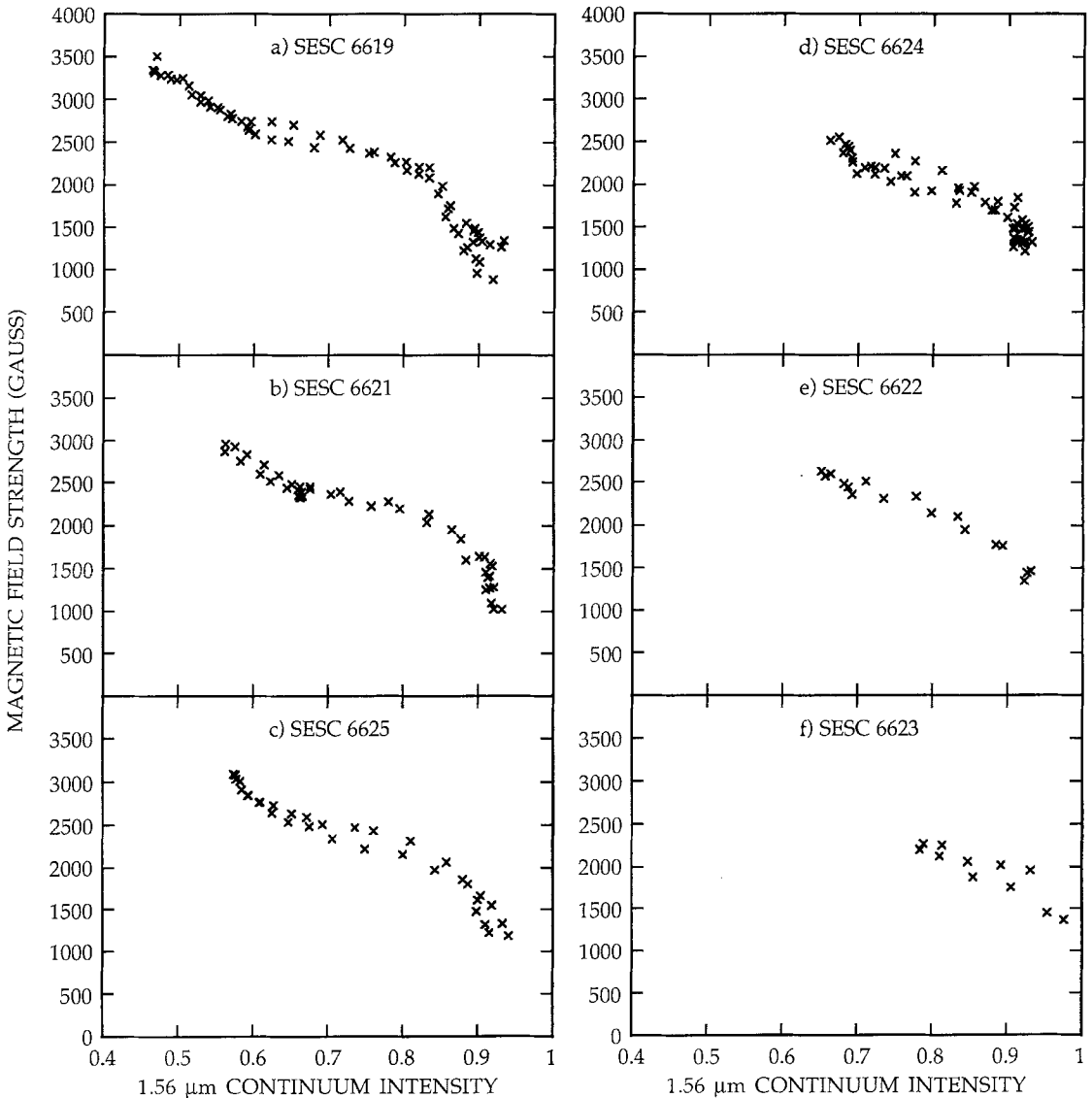


Fig. 3a-f. Magnetic field strength vs continuum intensity across each of six sunspots observed on 13 May, 1991. Parameters of the spots are given in Table I.

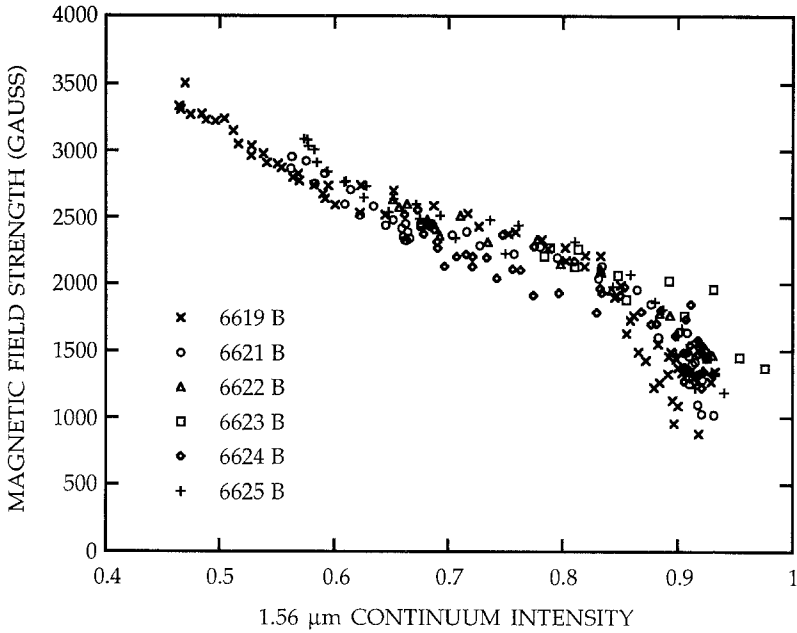


Fig. 4. Superposition of magnetic field strength vs continuum intensity for all six spots.

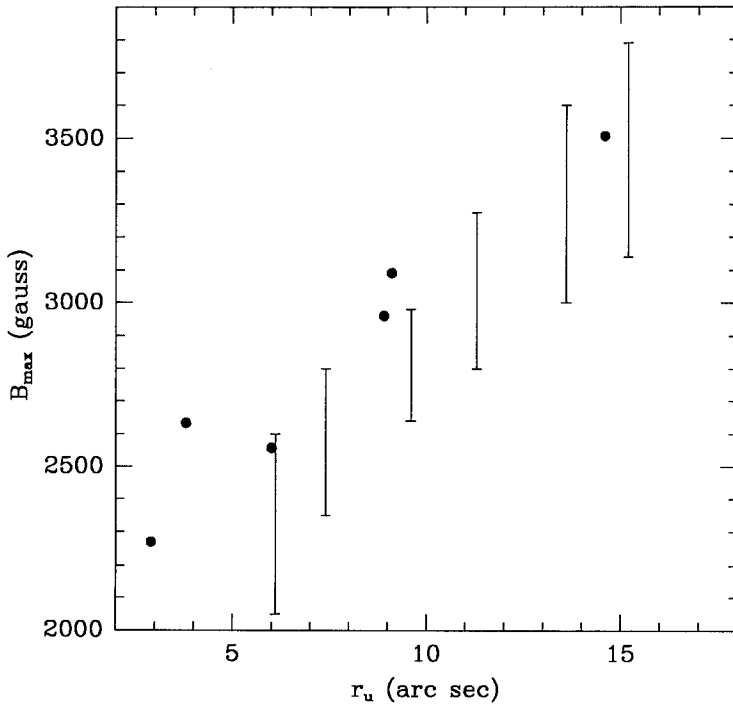


Fig. 5. Maximum magnetic field strength vs umbral radius. The points represent the six sunspots in the present sample. The vertical bars delimit the range of field strengths noted by Brants and Zwaan (1982).

intensities within smaller spots, possibly lowering the scatter in the figure, but the corrections should not change the nonlinear behavior of this relation. We hypothesize that this relationship is a general characteristic of sunspots.

Figure 5 shows maximum magnetic field B_{\max} vs average umbral radius r_u for all six spots. This agrees generally with the relation shown by Brants and Zwaan (1982) for spots of similar umbral size. The field strengths determined from the infrared data lie near the upper end of the ranges given by Brants and Zwaan; because the umbral σ -components of Fe I 1.5649 μm are formed 100–200 km lower than the σ -components of typical visible lines (Bruls, Lites, and Murphy, 1991), part of this effect may be attributed to a vertical field gradient of 0.5–1.0 G km^{-1} (Henze *et al.*, 1982). The infrared results support the conclusion of Brants and Zwaan (who exploited a purely umbral line of Ti I) that field strengths in all but the largest spots are typically underestimated by visible-light Fe I measurements because of stray light and blending of the π - and σ -components.

The relation between maximum magnetic field and the corresponding umbral intensity is shown in Figure 6. The strong trend toward smaller values of B_{\max} at higher values

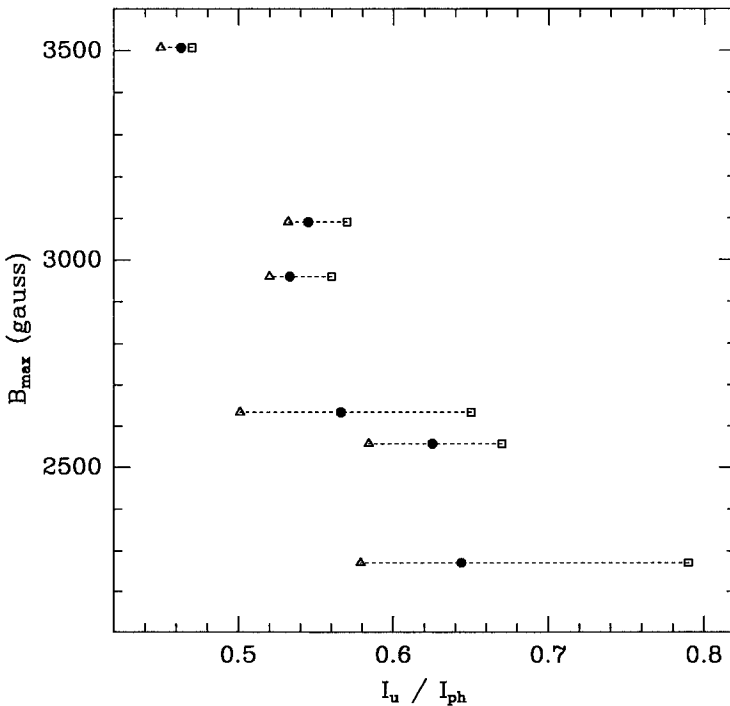


Fig. 6. Maximum magnetic field strength vs corresponding umbral intensity (in units of mean quiet Sun intensity) for the six sunspots. Three intensity values are shown for each spot: observed values (open squares); best-estimate stray light corrected values using the nominal blurring parameters (b_1, b_2, f_1, f_2) plus scattered light (see text) (filled circles); and worst-guess blurring parameters ($\tilde{b}_1, \tilde{b}_2, \tilde{f}_1, \tilde{f}_2$) plus scattered light (triangles).

of $I_{c,u}$ is clearly produced in part by the influence of blurred light in combination with the size vs field strength relationship of Figure 5. However, the trend is not entirely removed by the stray light corrections using the nominal parameters. Albreghsten and Maltby (1981) find no relation between B_{\max} and $I_{c,u}$ in the infrared. Although the stray light corrections in the present data are not ideal, the possibility of a significant B_{\max} vs $I_{c,u}$ relation deserves further investigation.

4. Discussion

Our central result is the characteristic, nonlinear relation between magnetic field strength and continuum intensity seen in Figures 2–4. The technical advantages of infrared sunspot measurements have revealed this relationship for – as far as we are aware – the first time. An obvious qualitative interpretation is that the umbra-penumbra transition is primarily a large change in temperature with radius, while the field strength changes comparatively little over the same radius interval. Most empirical expressions proposed for $B(r)$ make this assumption implicitly, since the umbral radius does not even appear as a parameter (Beckers and Schröter, 1969; Gurman and House, 1981; Adam, 1990).

Our result disagrees with the linear relation between field strength and continuum intensity proposed by Gurman and House (1981) for their 2000 G spot. We have used the Planck function to compare our I_c measurements at 1.56 μm with theirs near 630 nm, and we find that the B vs I_c plot at 630 nm has nearly the same shape as the infrared relation; in particular, the nonlinearity is undiminished. Moreover, a linear B vs I_c relation is inconsistent with the gently-sloping $B(r)$ profiles inferred from vector magnetograph observations (Kawakami, 1983; Lites and Skumanich, 1990), because the resulting $I_c(r)$ relation would lack a region of high gradient and there would be no subjective impression of an umbra-penumbra boundary. These smooth $B(r)$ relationships may, however, largely be an artifact of the low spatial resolution in the vector magnetograph measurements.

The flattening of the B vs I_c relation could be caused by spatially-unresolved inhomogeneities. The high-resolution observations of Lites, Scharmer, and Skumanich (1990) indicate that the magnetic field is not significantly weaker in bright penumbral filaments than in dark filaments – this alone implies an intrinsic nonlinear B vs I_c relation. One could also imagine unresolved, bright, non-magnetic regions to be present in sunspots; these would enhance the π -component of the observed spectra but not affect the position of the completely split σ -components, although it would decrease their amplitudes. In either of these extreme cases, the qualitative effect of bright, unresolved features would be to increase the measured continuum intensity without affecting the field strength. If these bright features were randomly distributed, an observed spatial element with a certain magnetic field strength could have a range of measured intensities, and we might expect more scatter in intensity than we see in Figures 2–4 for fields below about 2500 G. The actual relations for the best observed spots (Figure 3(a–c)) are instead rather smooth, with clearly distinguishable, continuous curves on opposite sides of the

center of the umbra. Thus, if the flattening of the B vs I_c relationship is caused by spatially-unresolved inhomogeneities, they must systematically depend on field strength or location within a sunspot in order to match the observed relation. Also, the effects of inhomogeneities should not be restricted to the penumbra, since fibrils (Livingston, 1991) and umbral dots (Lites *et al.*, 1991) could cause similar effects in sunspot umbrae. High spatial resolution infrared observations, able to resolve such inhomogeneities, could determine the magnetic field strength and its relation to intensity in the bright elements.

Our examination of selected $B(r)$ profiles reveals that, while the flattening of the B vs I_c curve in the penumbra is indeed mostly due to a steepening of $I_c(r)$, there is also in some cases a flattening of $B(r)$. This suggests that a single scale length (the penumbral radius) is not adequate to characterize $B(r)$. When $B(r)$ is not monotonic, we find that $I_c(r)$ usually follows $B(r)$ to preserve the B vs I_c relationship. This implies that a physical connection between magnetic field strength and temperature is fundamental, whereas relationships involving radius are merely average descriptions that may apply to unusually symmetric, 'theoretical' spots.

As has long been known (Alfvén, 1943; Schlüter and Temesváry, 1958), magneto-hydrostatic equilibrium,

$$(\nabla \times \mathbf{B}) \times \mathbf{B}/4\pi = \nabla P - \rho \mathbf{g}, \quad (3)$$

does establish relationships between magnetic field strength and the thermodynamic variables in a sunspot. For an axisymmetric, untwisted spot, the radial component of (3) is

$$\frac{\partial P}{\partial r} = \frac{B_z}{4\pi} \left(\frac{\partial B_r}{\partial z} - \frac{\partial B_z}{\partial r} \right), \quad (4)$$

where r is radius and z is depth in the atmosphere. Integrating Equation (4) between r and a field-free radius outside the spot, we obtain

$$P_e(z) - P(r, z) = B_z^2(r, z)/8\pi + \frac{1}{4\pi} \int_r^\infty B_z \frac{\partial B_r}{\partial z} dr', \quad (5)$$

where the subscript e denotes conditions in the field-free external photosphere. The last term in Equation (5) is the horizontal component of the magnetic tension force. Guided by analytic solutions for a few particular field configurations, Martínez Pillet and Vázquez (1990) rewrote (5) in the approximate form

$$P_e(z) - P(r, z) = [1 + f(r, z)]B^2(r, z)/8\pi, \quad (6)$$

such that departures from a purely vertical field are subsumed in the factor $f(r, z)$. The perfect gas law, $P = R\rho T/\mu$, may be used to write this as

$$\frac{T(r, z)}{T_e(z)} = \frac{\mu(r, z)}{\mu_e(z)} \frac{\rho_e(z)}{\rho(r, z)} \left[1 - \frac{1 + f(r, z)}{8\pi P_e(z)} B^2(r, z) \right]. \quad (7)$$

Del Toro Iniesta, Martínez Pillet, and Vázquez (1991) interpret this equation as a linear relationship between B^2 and T_b . However, it is clear from the r - and z -dependencies of the coefficients in Equation (7) that the relationship is only approximately linear. It should also be taken into account that neither $B(r)$ nor $T_b(r)$ is observed on a horizontal plane at depth z ; rather, each is measured on a curved surface of constant optical depth, and, since B is measured in a spectral line and T_b in the continuum, the two surfaces do not exactly coincide.

Putting aside these considerations for the moment, we repeat the data of Figure 2 in Figure 7 as a plot of B^2 vs T_b . Comparing Figure 2 with Figure 7, we cannot determine whether $\Delta T \sim \Delta B$ or $\Delta T \sim \Delta B^2$ in the umbra: there is not enough range in T_b to show much curvature. If we assume $\Delta T \sim \Delta B^2$ and use the slope of the umbral B^2 vs T_b relationship in Figure 7 in conjunction with Equation (7), setting $f = \rho/\rho_e = \mu/\mu_e = 1$ as a rough approximation, the required value of P_e corresponds to a depth $z \approx 800$ km in the convection zone model of Spruit (1974). We thus infer a plausible value for the Wilson depression, somewhat larger than the values reported by del Toro Iniesta, Martínez Pillet, and Vázquez (1991), which is not surprising since the infrared observations look deeper into the atmosphere.

The full value of spatially resolved measurements of field strength and temperature in sunspots cannot be realized with approximate representations such as Equation (7). Particularly in the penumbra, where the field may be predominantly horizontal, it is more

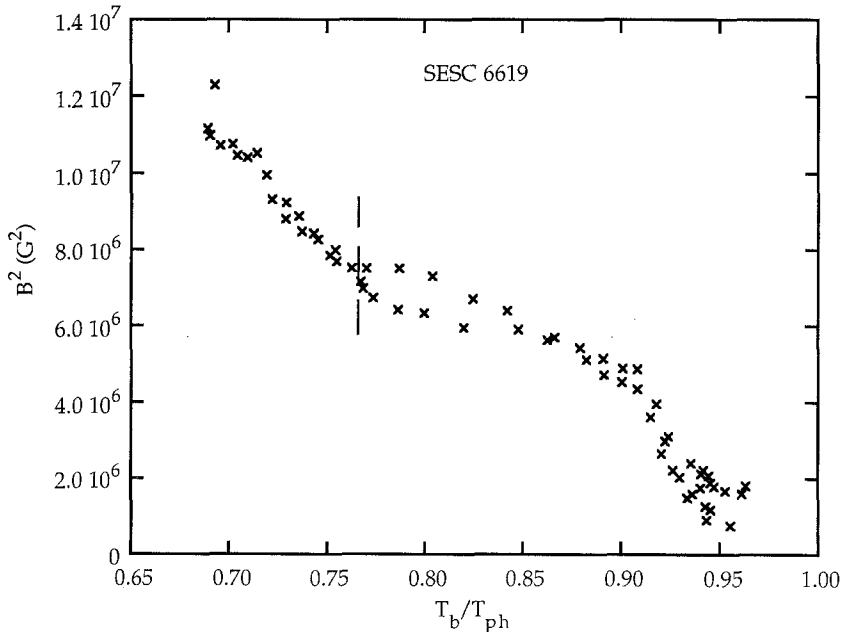


Fig. 7. Square of magnetic field strength vs brightness temperature (in units of photospheric temperature $T_{ph} = 6700$ K) for the large sunspot SESC 6619 (compare with Figure 2). The dashed line delineates the umbral region left of which the data are nearly linear.

accurate to retain the vertical component $B_z^2(r, z)$, as in Equation (5). It may be, in fact, that some of the rapid increase in T_b in the umbra-penumbra transition is due to a rapid decrease in B_z , and therefore $P_e - P(r)$, as the field inclines. Thus, magnetohydrostatic equilibrium considerations do not lead us to expect, nor do we observe, a purely linear relation between T_b and B or B^2 .

Further 1.5649 μm sunspot observations will measure magnetic field strength from Stokes V rather than I spectra. This will clarify the shape of the nonlinear, three-segment behavior in the B vs I_c relation and extend the results to the outer penumbra. We also intend to more fully exploit the two-dimensional nature of the observations.

Acknowledgements

We thank D. Jaksha, J. Wagner, C. Plymate, and P. Hartmann for their dedication during the observations. D. Lytle wrote the profile-fitting software. S. Solanki drew our attention to the early work of Alfvén. We also thank B. Lites for his comments as referee. This work was partially supported by NASA under Task 170-38-51-01-10.

References

- Adam, M. G.: 1990, *Solar Phys.* **125**, 37.
 Albreghsten, F. and Maltby, P.: 1981, *Solar Phys.* **71**, 269.
 Alfvén, H.: 1943, *Ark. Mat. Astron. Fys.* **29**, No. 11, 1.
 Beckers, J. M. and Schröter, E. H.: 1969, *Solar Phys.* **10**, 384.
 Brants, J. J. and Zwaan, C.: 1982, *Solar Phys.* **80**, 251.
 Bruls, J. H. M. J., Lites, B. W., and Murphy, G. A.: 1991, in L. November (ed.), *Solar Polarimetry*, Proc. 11th Sacramento Peak Workshop, NSO, Sunspot, New Mexico, p. 444.
 del Toro Iniesta, J. C., Martínez Pillet, V., and Vázquez, M.: 1991, in L. November (ed.), *Solar Polarimetry*, Proc. 11th Sacramento Peak Workshop, NSO, Sunspot, New Mexico, p. 224.
 Fowler, A. M., Probst, R. G., Britt, J. P., Joyce, R. R., and Gillett, F. C.: 1987, *Opt. Eng.* **26**, 232.
 Gurman, J. and House, L.: 1981, *Solar Phys.* **71**, 5.
 Harvey, J. W. and Hall, D.: 1975, *Bull. Am. Astron. Soc.* **7**, 459.
 Henze, W., Jr., Tandberg-Hanssen, E., Hagyard, M., Woodgate, B. E., Shine, R. A., Beckers, J. M., Bruner, M., Gurman, J. B., Hyder, C. L., and West, E. A.: 1982, *Solar Phys.* **81**, 231.
 Kawakami, H.: 1983, *Publ. Astron. Soc. Japan* **35**, 459.
 Lites, B. W. and Skumanich, A.: 1990, *Astrophys. J.* **348**, 747.
 Lites, B. W., Scharmer, G. B., and Skumanich, A.: 1990, *Astrophys. J.* **355**, 329.
 Lites, B. W., Bida, T. A., Johannesson, A., and Scharmer, G. B.: 1991, *Astrophys. J.* **373**, 683.
 Livingston, W.: 1991, *Nature* **350**, 45.
 Maltby, P., Avrett, E. H., Carlsson, M., Kjeldseth-Moe, O., Kurucz, R. L., and Loeser, R.: 1986, *Astrophys. J.* **306**, 284.
 Martínez Pillet, V. and Sánchez Almeida, J.: 1991, *Solar Phys.* **134**, 403.
 Martínez Pillet, V. and Vázquez, M.: 1990, *Astrophys. Space Sci.* **170**, 75.
 McPherson, M. R., Lin, H., and Kuhn, J. R.: 1992, *Solar Phys.* **139**, 255.
 Moore, R. and Rabin, D.: 1985, *Ann. Rev. Astron. Astrophys.* **23**, 239.
 Pierce, K.: 1991, *Solar Phys.* **133**, 215.
 Rabin, D.: 1992, *Astrophys. J.* **390**, L103.
 Schlüter, A. and Temesváry, S.: 1958, in B. Lehnert (ed.), 'Electromagnetic Phenomena in Cosmical Physics', *Proc. IAU Symp.* **6**, 263.
 Spruit, H.: 1974, *Solar Phys.* **34**, 277.
 Solanki, S. K.: 1991, private communication.

- Solanki, S. K., Biémont, E., and Mürset, U.: 1990, *Astron. Astrophys. Suppl. Ser.* **83**, 307.
- Staveland, L.: 1972, Oslo Inst. Theor. Astrophys. Rept. No. 36.
- Stenflo, J. O., Solanki, S. K., and Harvey, J. W.: 1987, *Astron. Astrophys.* **173**, 167.
- Vernazza, J. E., Avrett, E. H., and Loeser, R.: 1976, *Astrophys. J. Suppl.* **30**, 1.
- Vernazza, J. E., Avrett, E. H., and Loeser, R.: 1981, *Astrophys. J. Suppl.* **45**, 635.
- Wallace, L. and Livingston, W.: 1992, *An Atlas of a Dark Sunspot Umbral Spectrum from 1970 to 8640 cm⁻¹ (1.16 to 5.1 μ m)*, National Optical Astronomy Observatories, Tucson.
- Zwaan, C.: 1965, *Rech. Astron. Obs. Utrecht.* **17**, part 4.
- Zwaan, C.: 1968, *Ann. Rev. Astron. Astrophys.* **6**, 135.